The structure and terahertz dynamics of water confined in nanoscale pools in salt solutions

David A. Turton,[ab] Carmelo Corsaro,[c] Marco Candelaresi,[a] Angela Brownlie,[d] Ken R. Seddon,[d] Francesco Mallamace[ce] and Klaas Wynne*[ab]

Received 26th November 2010, Accepted 11th January 2011
DOI: 10.1039/c0fd00005a

The behaviour of liquid water below its melting point is of great interest as it may hold clues to the properties of normal liquid water and of water in and on the surfaces of biomolecules. A second critical point, giving rise to a polyamorphic transition between high and low density water, may be hidden in the supercooled region but cannot be observed directly. Here it is shown that water can be locked up in nano-pools or worm-like structures using aqueous LiCl salt solutions and can be studied with terahertz spectroscopies. Very high dynamic range ultrafast femtosecond optical Kerr effect (OKE) spectroscopy is used to study the temperature-dependent behaviour of water in these nano-pools on timescales from 10 fs to 4 ns. These experiments are complemented by temperature-dependent nuclear magnetic resonance (NMR) diffusion measurements, concentration-dependent Fourier-transform infrared (FTIR) measurements, and temperature-dependent rheology. It is found that liquid water in the nanoscale pools undergoes a fragile-to-strong transition at about 220 K associated with a sharp increase in the inhomogeneity of translational dynamics.

Introduction

Liquid water and its complex crystallisation and vitrification behaviour has been studied for at least 235 years.[1] Despite this, many of the strange properties of liquid water—such as its density maximum at 4 °C or its increasing heat capacity on cooling below the melting point—remain unexplained.[2–5] In the 1970s, Speedy and Angell suggested that the approach of the limit of mechanical stability for the supercooled liquid phase at ~220 K (at atmospheric pressure) could explain many of the odd behaviours of water.[6] An alternative approach was developed by Poole *et al.* and invokes the existence of a second critical point that terminates a coexistence line between low- and high-density amorphous phases of (glassy) water.[4,7,8] Unfortunately, this second critical point (if it exists) and the associated polyamorphic transition is difficult to study as it lies below the homogeneous nucleation temperature in a region known as "no man's land".[5,9] A number of recent studies of nanoconfined water have suggested that water does indeed undergo a transition at 220–230 K from fragile (strongly glass forming) to strong (near Arrhenius behaviour).[10–19] Although,

[a]*School of Chemistry, WestCHEM, University of Glasgow, UK. E-mail: klaas.wynne@glasgow.ac.uk*
[b]*Dept. of Physics, SUPA, University of Strathclyde, Glasgow, UK*
[c]*Dipartimento di Fisica, Universita di Messina, Italy*
[d]*School of Chemistry and Chemical Engineering, Queen's University Belfast, UK*
[e]*Dept. of Nuclear Science and Engineering, Massachusetts Institute of Technology, Cambridge, USA*

these studies have generated considerable controversy,[20–22] there is evidence to believe that the influence of the second critical point extends all the way into the normal liquid region up to the boiling point.[23] Here, we show that ultrafast terahertz spectroscopies may be used to shed a novel light on this issue.

In our studies, water was "nanoconfined" by using aqueous salt solutions.[24,25] Recent work[10] has suggested that mixtures of liquids may lead to nanometre scale percolation networks in which liquid water may be supercooled into no man's land without crystallisation. In our studies, a eutectic solution of LiCl in water, corresponding to a concentration of 6.8 M,[26,27] was used. This eutectic mixture can be cooled to 200 K without crystallisation and readily forms a glass at lower temperatures.[28] Ultrafast optical Kerr-effect (OKE) spectroscopy was used to study these samples as OKE experiments are, in this case, only sensitive to the motions of water.[25] The presence of the 65 and 180 cm^{-1} TA and LA "phonon" bands[29] of water (corresponding to the hydrogen-bond bend and stretch modes) demonstrates the presence of liquid water pools. This is confirmed by FTIR spectroscopy of the OH-stretch band of water.

Dynamic measurements from 10 fs to 4 ns show an increase of the translational[25,30] relaxation time upon cooling that, in contrast with previous results,[30,31] is consistent with a (super-Arrhenius) Vogel-Fulcher-Tammann curve with a critical temperature of $\sim$140 K. Fitting these data with a stretched-exponential function reveals a dramatic increase in the liquid *heterogeneity* below 220 K. Comparing these results with measurements of macroscopic viscosity and NMR diffusion[10] provides new insight into the behaviour of water near the putative second critical point.

Experimental

Studies were performed using ultrafast optical Kerr-effect (OKE) spectroscopy, nuclear magnetic resonance (NMR) diffusion measurements, Fourier-transform infrared (FTIR) spectroscopy, and macroscopic rheology.

OKE

OKE spectroscopy is the time-domain variant of anisotropic Raman scattering and measures the time correlation function of the anisotropic part of the polarisability tensor.[32–35] As monatomic ion salts have neither an anisotropic atomic polarisability nor a permanent dipole moment, they make a minimal direct contribution to the OKE spectrum allowing the change in behaviour of the water alone to be observed. However, the molecular polarisability tensor of water itself is nearly isotropic with a vanishingly small anisotropic component.[36,37] As a result, the OKE signal is very weak and the lowest frequency part of the OKE spectrum (or the slowest decay in the time domain) is not due to rotational diffusion but due to collision-induced effects representing translational motions within the first solvation shell.[25,30,37,38] In this study, we are mostly interested in these relatively slow (about 1 ps in pure water at room temperature[38]) translational motions and the manner of their decay. As these signals are exceedingly weak compared to faster electronic and librational responses of water[30,38–45] they are difficult to measure accurately with spontaneous Raman scattering,[46,47] and a large dynamic range time-domain OKE signal is required. To achieve this, two experimental set-ups have been used.

A high time resolution experimental set-up for OKE measurements has been described previously[35,48,49] and uses 800-nm 24-fs (FWHM) $sech^2$ pulses with 8 nJ per pulse at a repetition rate of 76 MHz. The beam is split into pump and probe beams (9 : 1), which are co-focused by a 10-cm focal length achromat into the sample contained in a 2-mm-pathlength quartz cuvette held in a cryostat (Oxford Instruments, *Optistat DN*). An optical delay line with a resolution of 500 nm (3.3 fs) and a maximum delay of 4 ns introduces a variable pump–probe time delay. The OKE signal is measured by a balanced-detection technique described

previously.[50,51] This was complemented by a second similar set-up using a regenerative amplifier producing 800-nm 23-fs (FWHM) sech^2 pulses with 2.5 mJ per pulse at a repetition rate of 1 kHz. For OKE experiments, the pulses were stretched to obtain a 1-ps pulse duration and attenuated to 2.5 μJ. This low-repetition rate set-up produces OKE signals with lower signal-to-noise ratio but greater dynamic range. The data from the two set-ups overlap well between typically 1 and 10 ps allowing them to be merged into a single data set with, for the salt solution, a dynamic range of *circa* 6 orders of magnitude and a time delay range from femtoseconds to 4 ns (see Fig. 1).

NMR

In the case of liquid water, OKE measures translational motion in and out of the first solvation shell through collision-induced effects. Complementary pulsed field gradient NMR diffusion measurements were performed that report on the macroscopic self-diffusion coefficient (D_S) and the average translational relaxation time. These experiments have been described in detail previously for water on proteins,[11] water confined to nanopores,[12–14] and water–methanol mixtures.[10] In particular, here we have used a maximum gradient amplitude of 50 G cm^{-1}, a gradient pulse duration from 1 to 7 ms, and a diffusion time from 100 to 800 ms.

Infrared spectroscopy

Infrared spectroscopy was performed using a Bruker Vertex 70 spectrometer using a Harrick MVP2 diamond attenuated total reflection (ATR) unit. The spectrometer has two beam splitters and two room-temperature DTGS detectors allowing us take spectra from ~30 cm^{-1} upwards. The spectra were obtained at room temperature with a resolution of 4 cm^{-1}.

Viscosity

Rheological measurements were performed using two set-ups. Bulk viscosity measurements were carried out using a Cambridge Viscosity VISCOlab 3000 from room temperature to about −40 °C with a viscosity range of 0.1–100 cP. Using a Bohlin Gemini II Rheometer with extended temperature chamber, additional measurements down to −150 °C were made in the range 15–10 000 cP.

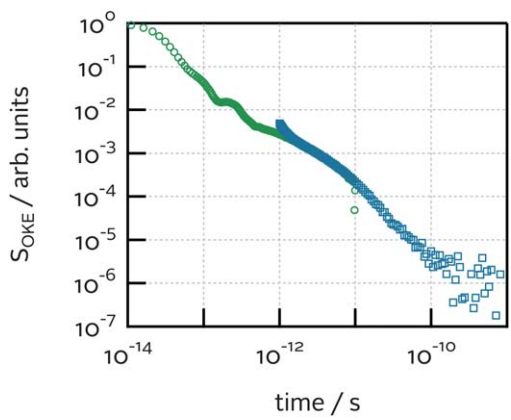

Fig. 1 The optical Kerr effect (OKE) data were obtained with two set-ups using 24-fs low-energy pulses (green circles) and 1-ps high-energy pulses (blue squares). Data from the two set-ups are patched by overlapping between 1 and 10 ps.

Samples

Samples were prepared using anhydrous LiCl and deionised water (Sigma-Aldrich). A stock solution of LiCl in water was prepared at a concentration of 13.24 M determined using Mohr's method. Samples at concentrations of 3.02, 5.62, 6.76, 9.03, and 11.03 M were prepared from this stock solution by dilution with water. The 6.76 M solution was used for OKE, NMR, and viscosity measurements. The 6.76 M solution is known to be at the eutectic concentration[27] and corresponds to a solution of water with 25 mass% LiCl, 7.86 mol kg^{-1}, and 7 water molecules per LiCl. The solubility of LiCl in water is >35 mol% at 273 K.

Results and discussion

OKE

Fig. 2 shows OKE data taken on a 6.76 M eutectic mixture of LiCl and water at a range of temperatures. The eutectic mixture can be cooled to about 190 K, remaining a liquid without crystallisation, while at 130 K it forms an optically transparent glass. In the time domain, one can see a peak due to the electronic polarisability, oscillations caused by underdamped vibrational and librational modes, followed by a slower decay. As the temperature is lowered, the slower decay slows down while becoming increasingly stretched (approaching a straight line on a log-log plot). Only after the relaxation has decayed over several orders of magnitude does the decay become exponential (curved down on a log-log plot). These data can be analysed more conveniently in the frequency domain after deconvolution to take into account the finite width of the laser pulse.

The OKE spectra below 10 THz (300 cm^{-1}) show three clear bands (see Fig. 2). Above 10 THz are three bands at *ca.* 400 cm^{-1} and 800 cm^{-1} representing the three librational motions of the water molecule. However, because the OKE signal of water is so weak, the shape and amplitude of these bands in the OKE spectrum are generally unreliable.[29,52] The relaxational mode that occurs at ~10 cm^{-1} (330 GHz) in neat water at room temperature,[25,38] and which is predominantly of translational origin, is strongly temperature dependent. This relaxational mode shifts to lower frequency (~100 GHz) in the eutectic salt solution consistent with the previously reported slowdown of translational motions in aqueous electrolyte solutions due to the formation of nano-pools.[25,53] At higher frequency, two bands are readily identified and in Raman studies have been assigned[29] to the transverse acoustic (TA)

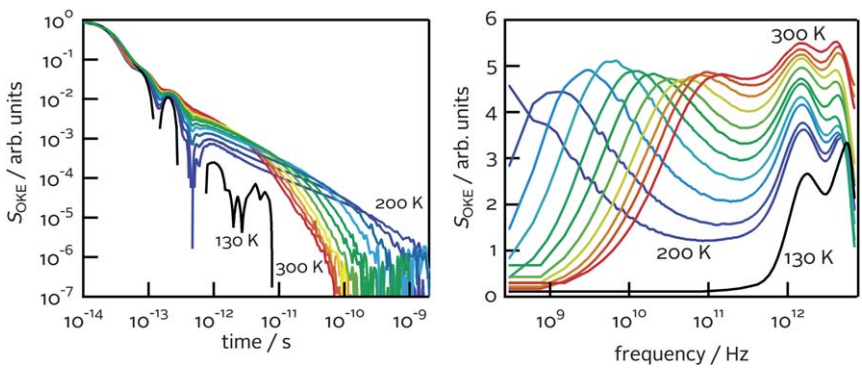

Fig. 2 Ultrafast OKE data on a 6.76 M eutectic mixture of LiCl and water at a range of temperatures. (left) OKE data on logarithmic axes in the time-domain taken at a range of temperatures from 200 K (blue) to 300 K (red) in steps of 10 K, and at 130 K (black). (right) OKE data Fourier analysed and deconvolved resulting in a reduced anisotropic Raman spectrum. The horizontal (frequency) axis is logarithmic.

mode at ~60 cm^{-1} (2 THz) and the longitudinal acoustic (LA) mode at ~180 cm^{-1} (6 THz) in terms of the phonon modes of the crystalline state. Alternatively, and more simply, these modes have been interpreted as the transverse and longitudinal stretches of a hydrogen-bonded O–O–O motif or of the "Walrafen" tetrahedral pentamer of water.

As the sample is cooled down, the TA and LA modes of water remain approximately at the same frequency while becoming narrower.[54] The relaxational mode shifts to lower frequency on cooling. In the glass sample at 130 K, the TA and LA modes of water remain while the relaxational mode has been frozen out. The latter spectrum has a "diffusive tail" below 500 GHz, which will be discussed elsewhere.[54]

The OKE data are fit in the time domain with a number of anti-symmetrised Gaussians representing the TA and LA modes and the librations. The relaxational mode, which is of greatest interest here, can be fit with (the derivative of) a stretched exponential (or Kohlrausch–Williams–Watts) function[38]

$$S_{\mathrm{OKE}} \propto (\mathrm{d}/\mathrm{d}t)\mathrm{e}^{-(t/\tau)^{\beta}} \quad (1)$$

where τ is the relaxation time and $0 < \beta \leq 1$ the stretching parameter. Following Mamontov,[55] one can define an average relaxation time as $\langle\tau\rangle = (\tau/\beta)\Gamma(\beta^{-1})$ or alternatively as

$$\langle\tau\rangle = \int_0^\infty \mathrm{d}t\ t\ \mathrm{e}^{-(t/\tau)^{\beta}} / \int_0^\infty \mathrm{d}t\ \mathrm{e}^{-(t/\tau)^{\beta}} = \tau\ \Gamma(2\beta^{-1})/\Gamma(\beta^{-1}) \quad (2)$$

where $\Gamma(x)$ is the gamma function but in practice τ and $<\tau>$ differ little for the values of β relevant here.

Fig. 3 shows the τ and β fit parameters (as well as $<\tau>$) as a function of temperature. The relaxation time does not follow an Arrhenius dependence but instead varies more steeply with temperature. The β fit parameter is, within experimental error, constant at high temperature at $\beta \approx 0.6$. In pure water, it has previously been measured[30] as $\beta = 0.6$ and even in the simplest noble-gas liquids, where translational motions are also probed, its value has been measured as $\beta = 0.66$.[35,53] Below $T = 220$ K (above $1000/T = 4.5$), the value of β falls sharply corresponding to the increase in stretching seen in the time-domain data in Fig. 2.

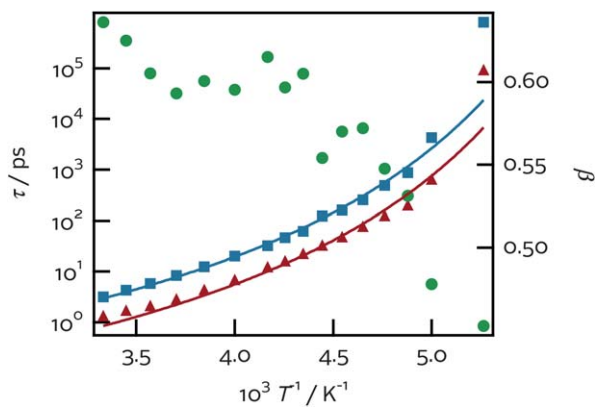

Fig. 3 Results of fitting (the derivative of) a stretched exponential relaxation function to the temperature dependent OKE data of a eutectic aqueous LiCl solution. The relaxation time τ is shown as red triangles, the average relaxation time $<\tau>$ as blue squares, and the stretching parameter β as green circles. The solid curves are based on a Stokes–Einstein expression (with an additional scaling factor) while using a Vogel-Fulcher-Tammann fit for the viscosity with $D = 4.0$ and $T_0 = 143$ K.

FTIR

Infrared spectra of water and aqueous LiCl solutions were obtained using FTIR ATR spectroscopy. The ATR spectra show isosbestic points on the OH-stretch ($\sim$3400 cm^{-1}), bend ($\sim$1600 cm^{-1}), and librational ($\sim$600 cm^{-1}) bands consistent with the presence of two distinct species, bulk and bound water. The ATR spectra were converted to absorption spectra using a numerical Kramers–Kronig transform.[56] The result for the OH-stretch band is shown in Fig. 4, while the low-frequency part of the spectrum will be discussed elsewhere.[54] For increasing LiCl concentration, the OH-stretch band narrows and shifts to a higher frequency. Two isosbestic points in this band (as well as elsewhere in the spectrum) show that this is caused by the conversion between two species consistent with previous analyses.[57] Analysis of the aqueous LiCl data here suggests that the concentration of bulk water decreases approximately linearly with a zero concentration intercept at 15.5 M.

Viscosity

Fig. 5 shows the temperature dependent viscosity of the eutectic mixture. Based on the original work of Taborek *et al.* and others, it is generally accepted that the viscosity of water[6,31,58] and aqueous solutions[59] follows a power law. This has been related to the suggested existence of a thermodynamic singularity at $T \approx 220$ K by Speedy and Angell.[6] Such power-law dependencies also follow from mode-coupling theories (MCTs). Thus, the viscosity is assumed to be of the form

$$\eta = B + \frac{A}{(T - T_S)^{\gamma}} \tag{3}$$

where T_S is the temperature of the singularity. However, the data shown in Fig. 5 are not consistent with this behaviour. If only the high temperature part is fit by the MCT expression, a singularity temperature of $T_S = 203 \pm 43$ K and a critical exponent $\gamma = 2.3 \pm 1.7$ are found as is consistent with measurements on pure water in the high temperature range.[30,60] However, the data agree with the Vogel–Fulcher–Tammann expression

$$\eta = A\exp\left(\frac{DT_0}{T - T_0}\right) \tag{4}$$

over the entire temperature range with $A = 0.09$, $D = 4.0 \pm 1.7$ and $T_0 = 143 \pm 14$ K again consistent with neat water.[60] As $D < 10$, the eutectic mixture is fragile (non-Arrhenius), which is typical of good glass formers.

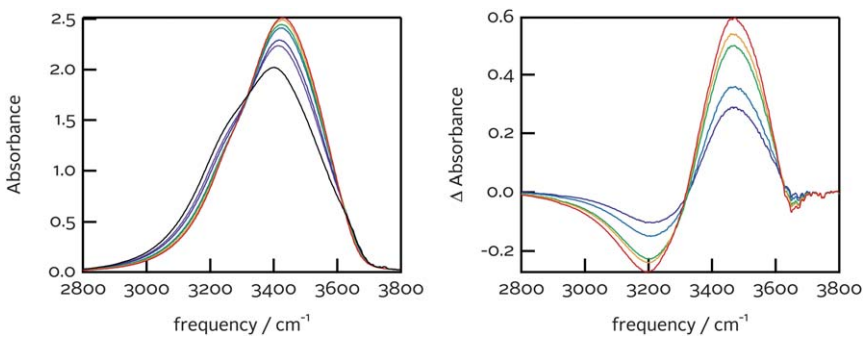

Fig. 4 (left) Absorbance spectra of aqueous LiCl solutions in the OH stretching region at concentrations ranging from 3.02 M (purple) to 13.24 M (red). The spectrum of pure water is shown in black. (right) Idem, water spectrum subtracted.

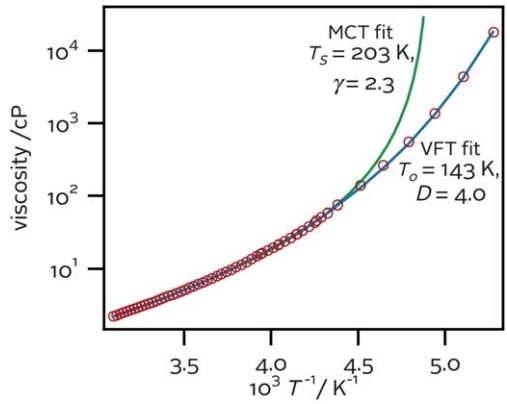

Fig. 5 Viscosity (red circles) of 6.76 M aqueous LiCl solution measured using two set-ups (see text). High temperature data has been multiplied by 1.8 to match the low temperature data over the range $1000/T = 3.9$ to 4.3. The blue curve is the VFT fit, and the green curve is the MCT expression (see text).

NMR

Fig. 6 shows an Arrhenius plot of NMR diffusion measurements of the macroscopic diffusion coefficient of protons in the eutectic aqueous LiCl solution as a function of temperature. Previous similar measurements on water confined to nano-pores, protein hydration water, and water–alcohol mixtures[10–19] have reported a change in behaviour from strong (Arrhenius) to fragile (non-Arrhenius) at $1000/T \cong 4.5$. Such a change is not obviously visible here probably because the mixing time between water molecules belonging to the solvation shell and to the bulk is much faster than the NMR diffusion time. So NMR macroscopic diffusion is averaged over the two different species of water.

Discussion and conclusion

The concentration of LiCl in the eutectic mixture with water is high, corresponding to only seven water molecules per LiCl, hence it is reasonable to ask whether there is

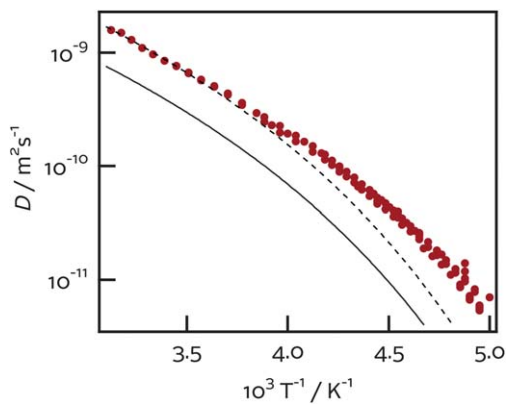

Fig. 6 NMR diffusion measurements of the macroscopic diffusion coefficient as a function of temperature (red circles). The black line is a calculation of the diffusion coefficient based on the measured macroscopic viscosity (see Fig. 5) and a radius for the water molecule of 0.14 nm. The dashed line uses a viscosity scaled by 0.45.

still "bulk" water in the system.[61] Solvation of salts and in particular the lithium cation has been studied extensively, but there are still strong divisions of opinion, from both simulation and experimental studies, as to coordination number and to the effect of solvated ions on the structure and dynamics of water.[24,62–67] There is increasing consensus that in relatively concentrated solution the Li ion is solvated by a shell of 3–4 water molecules with a residence time of hundreds of picoseconds. These water molecules are still able to take part in hydrogen bonding with the surrounding water and both the Li and Cl ions are at the middle of the Hofmeister series implying a minimal effect on structure.

There are several pieces of experimental evidence demonstrating the presence of bulk water in the concentrated LiCl solutions studied here. Dielectric relaxation spectroscopy on LiCl solutions[68,69] and recent time-domain terahertz spectroscopy (THz-TDS) experiments on concentrated LiCl solutions[70] have shown that the rotational relaxation time of water is essentially unaltered, as has also been shown for NaCl and $MgCl_2$ solutions.[25] Of course, such studies do show a reduction of the dielectric constant with increasing salt concentration, consistent with the ions (particularly the cations) immobilising an increasing fraction of the water molecules.

The OKE data presented here possibly provide the strongest evidence for bulk water. The OKE spectrum in Fig. 2 shows the bands peaking at $\sim$60 and 180 cm^{-1} corresponding to the LA and TA phonon modes of liquid water. These bands are known[71] to be strongly altered in crystalline and glassy (both low and high density amorphous) phases. That this fingerprint of bulk water still dominates the spectrum of the eutectic solution strongly implies the presence of bulk water. In fact, in Fig. 2 the apparent reduction in intensity of the LA and TA phonon bands is mostly due to the shift of the relaxational band to lower frequency. It is also seen that, at room temperature, the relaxational band in 6.76 M LiCl solution is shifted to lower frequency compared to in neat water. This is the same behaviour seen in NaCl and $MgCl_2$ solutions and consistent with the presence of nano-pools of water.[25]

These results are consistent with our measurements of the infrared spectrum and in particular the OH-stretch band of water. The OH-stretch band shows isosbestic points consistent with the conversion of bulk water into water bound to the lithium cation. Analysis of the infrared data shows that in the 6.76-M eutectic solution 45% of the water molecules are bound while 55% remains free (bulk). The eutectic mixture is well away from the saturation concentration ($\sim$13.5 M at room temperature[27]) and there is no evidence for inhomogeneities such as the clustering of LiCl.

Thus, there is experimental evidence for the existence of nanometre-sized water pools or the "worm-hole" structure proposed by Angell[72] and similar to emulsified water.[9] It cannot be excluded that some water molecules, hydrogen-bound to the ions, appear as mobile in some spectroscopies.[24] *Ab initio* molecular dynamics simulations suggest that even at a concentration of 14 M there may be pairs of hydrogen-bound water molecules one of which is in the first solvation shell of Li^+.[67] However, the lack of change in the rotational–relaxation time as a function of LiCl concentration seen in THz-TDS,[70] which measures the tumbling of the permanent dipole moment, combined with the observation of the LA and TA phonon modes in OKE is strong evidence for nano-pools of "bulk" water.[25,53]

When a liquid or solution exhibits nanometre scale *meso*-structuring, one may expect the macroscopic viscosity and the effective microscopic viscosity to become decoupled.[48] The macroscopic viscosity is influenced by the density of the mesoscopic structures (as in Einstein's viscosity of a dilute suspension of hard spheres), with a divergence in the viscosity expected as the packing fraction of mesoscopic structures approach a critical packing fraction or jamming transition.[53,73] The microscopic viscosity is that experienced by the water molecules in the nano-pools. Thus, one might expect a breakdown of the Stokes–Einstein and Stokes–Einstein–Debye expression for translational and rotational diffusion leading to a fractional Stokes–Einstein (Stokes–Einstein–Debye) relation.[8,49,74,75]

The Stokes–Einstein and Stokes–Einstein–Debye equations for translational and rotational diffusion of a probe particle immersed in a solvent are[38]

$$D_{\text{trans}} = \frac{k_B T}{6\pi\eta R}, D_{\text{rot}} = \frac{k_B T}{8\pi\eta R^3} \quad (5)$$

where T is the temperature, η the (macroscopic) shear viscosity, and R the radius of the diffusing object. The latter expression can be related to rotational diffusion time t_n as[40,75,76]

$$t_n = \frac{6}{n(n+1)} \frac{V\eta}{k_B T} \quad (6)$$

where $V = \frac{4}{3}\pi R^3$ and n relates to the type of spectroscopy and is typically 1 (for dielectric relaxation spectroscopy and linear infrared spectroscopy) or 2 (for four-wave mixing experiments such as OKE, infrared pump–probe, fluorescence, *etc.*). Applying the Stokes–Einstein–Debye equation to room temperature water ($\eta = 1$ cP),[77] one estimates a molecular radius of $R = 0.193$ nm and a rotational relaxation time of $t_2 = 7.4$ ps, which is in reasonable agreement with the 2.6 ps measured with infrared pump–probe spectroscopy.[24] By decreasing the effective radius of the water molecule to $R = 0.14$ nm, one matches the experimental t_2. The viscosity measured in the eutectic solution at room temperature is 4 cP from which one predicts $D_{\text{trans}} = 3.8 \times 10^{-10}$ m s^{-2}, which is a factor of 2.2 lower than that measured (see Fig. 6) indicating a small fractional Stokes–Einstein effect at room temperature.

The experimental temperature-dependent viscosity (Fig. 5) follows a Vogel–Fulcher–Tammann dependence with a critical temperature of 143 K. This is very close to the experimental glass transition temperature of water and aqueous LiCl solutions.[5,26,78,79] The measured temperature-dependent viscosity can now be used to predict the temperature-dependent translational diffusion coefficient. This is shown as the solid line in Fig. 6, which differs by about a factor of 2.2 as discussed above. The dashed line in Fig. 6 is scaled by a factor of 2.2. It then matches the diffusivity data closely up to $1000/T \approx 4$ where it then diverges. This is evidence for a subtle change of behaviour similar to the fragile-to-strong transition observed in confined water. Previous measurements on water confined to nano-pores, protein hydration water, and water-alcohol mixtures[10–19] have similarly reported a fragile-to-strong transition at $1000/T \cong 4.5$. Here two effects are observed masking the transition: a fractional Stokes–Einstein effect caused by the salt-induced nano-structuring (which is temperature independent) combined with a fragile-to-strong transition in the water nano-pools (which appears as a temperature-dependent deviation from Arrhenius behaviour). This is consistent with previous observations in methanol–water mixtures[10] and a possible observation of change in behaviour in LiCl solutions observed with Brillouin light scattering[80,81] and neutron scattering.[19,55]

The slowest relaxation in the OKE data is a collision-induced signal and thus corresponds to translational motions. This is similar to the NMR diffusion measurements but on a shorter length scale: in and out of the first solvation shell rather than averaged. The measured temperature-dependent macroscopic viscosity can again be used to predict the temperature-dependent OKE translational dynamics. This is shown as the solid lines in Fig. 3. Note that there is no simple analytical expression relating macroscopic viscosity to the timescale of movement in and out of the first solvation shell. Hence, we have used the Stokes–Einstein expression and scaled it to match the OKE relaxation time and average relaxation time at high temperature. The prediction matches the OKE relaxation data closely at high temperature with some deviation at low temperature above $1000/T \approx 5$.

However, the most dramatic change is in the temperature-dependent stretching coefficient β, which falls from its normal value of 0.6 to 0.45 around $1000/T \approx 4.5$. The dramatic effect this has can be seen clearly in the time-domain data in

Fig. 2, where the decay is seen to take on a distinct power-law decay form at low temperature.

A stretched-exponential decay with $\beta < 1$ implies an inhomogeneous distribution of decay times and hence environments. As we have shown previously, a certain degree of inhomogeneity is already present in the simplest of liquids: the noble-gas liquids exhibit a decay with $\beta = 0.66$.[35] A similar stretched decay is observed in liquid water[35] and supercooled water.[30] In the eutectic aqueous LiCl solution, we find that the stretching parameter decreases dramatically at $T = 220$–230 K implying an increase in the heterogeneity of the water in the nano-scale pools. The experiments presented here cannot distinguish the origin of this inhomogeneity. Our experiments also only measure changes in the dynamics of translation and ignore rotations. Thus, it would be very interesting to perform matching experiments using dielectric relaxation spectroscopy[68] or terahertz time-domain spectroscopy to temperatures well below 220 K.

Acknowledgements

We gratefully acknowledge the Engineering and Physical Sciences Research Council (EPSRC) for funding this project.

References

1 J. Black, *Philos. Trans. R. Soc. London*, 1775, **65**, 124–128.
2 H. E. Stanley, P. Kumar, S. Han, M. G. Mazza, K. Stokely, S. V. Buldyrev, G. Franzese, F. Mallamace and L. Xu, *J. Phys.: Condens. Matter*, 2009, **21**, 504105.
3 I. Brovchenko and A. Oleinikova, *ChemPhysChem*, 2008, **9**, 2660–2675.
4 P. Debenedetti, *J. Phys.: Condens. Matter*, 2003, **15**, R1669–R1726.
5 C. A. Angell, *Science*, 2008, **319**, 582–587.
6 R. Speedy and C. Angell, *J. Chem. Phys.*, 1976, **65**, 851–858.
7 P. Poole, F. Sciortino, U. Essmann and H. Stanley, *Nature*, 1992, **360**, 324–328.
8 H. E. Stanley, S. V. Buldyrev, G. Franzese, P. Kumar, F. Mallamace, M. G. Mazza, K. Stokely and L. Xu, *J. Phys.: Condens. Matter*, 2010, **22**, 284101.
9 O. Mishima, *J. Chem. Phys.*, 2010, **133**, 144503.
10 F. Mallamace, C. Branca, C. Corsaro, N. Leone, J. Spooren, H. E. Stanley and S.-H. Chen, *J. Phys. Chem. B*, 2010, **114**, 1870–1878.
11 M. Lagi, X. Chu, C. Kim, F. Mallamace, P. Baglioni and S.-H. Chen, *J. Phys. Chem. B*, 2008, **112**, 1571–1575.
12 S.-H. Chen, F. Mallamace, C.-Y. Mou, M. Broccio, C. Corsaro, A. Faraone and L. Liu, *Proc. Natl. Acad. Sci. U. S. A.*, 2006, **103**, 12974–12978.
13 F. Mallamace, M. Broccio, C. Corsaro, A. Faraone, U. Wanderlingh, L. Liu, C. Mou and S. Chen, *J. Chem. Phys.*, 2006, **124**, 161102.
14 F. Mallamace, M. Broccio, C. Corsaro, A. Faraone, L. Liu, C.-Y. Mou and S.-H. Chen, *J. Phys.: Condens. Matter*, 2006, **18**, S2285–S2297.
15 A. Faraone, K.-H. Liu, C.-Y. Mou, Y. Zhang and S.-H. Chen, *J. Chem. Phys.*, 2009, **130**, 134512.
16 Y. Zhang, M. Lagi, E. Fratini, P. Baglioni, E. Mamontov and S.-H. Chen, *Phys. Rev. E: Stat., Nonlinear, Soft Matter Phys.*, 2009, **79**, 040201.
17 J. Mattsson, R. Bergman, P. Jacobsson and L. Borjesson, *Phys. Rev. B: Condens. Matter Mater. Phys.*, 2009, **79**, 174205.
18 X.-Q. Chu, A. I. Kolesnikov, A. P. Moravsky, V. Garcia-Sakai and S.-H. Chen, *Phys. Rev. E: Stat., Nonlinear, Soft Matter Phys.*, 2007, **76**, 021505.
19 E. Mamontov, D. R. Cole, S. Dai, M. D. Pawel, C. D. Liang, T. Jenkins, G. Gasparovic and E. Kintzel, *Chem. Phys.*, 2008, **352**, 117–124.
20 W. Doster, S. Busch, A. M. Gaspar, M.-S. Appavou, J. Wuttke and H. Scheer, *Phys. Rev. Lett.*, 2010, **104**, 098101.
21 S. Pawlus, S. Khodadadi and A. P. Sokolov, *Phys. Rev. Lett.*, 2008, **100**, 108103.
22 M. Vogel, *Phys. Rev. Lett.*, 2008, **101**, 225701.
23 C. Huang, K. T. Wikfeldt, T. Tokushima, D. Nordlund, Y. Harada, U. Bergmann, M. Niebuhr, T. M. Weiss, Y. Horikawa, M. Leetmaa, M. P. Ljungberg, O. Takahashi, A. Lenz, L. Ojamae, A. P. Lyubartsev, S. Shin, L. G. M. Pettersson and A. Nilsson, *Proc. Natl. Acad. Sci. U. S. A.*, 2009, **106**, 15214–15218.

24 K. J. Tielrooij, N. Garcia-Araez, M. Bonn and H. J. Bakker, *Science*, 2010, **328**, 1006–1009.
25 D. A. Turton, J. Hunger, G. Hefter, R. Buchner and K. Wynne, *J. Chem. Phys.*, 2008, **128**, 161102.
26 C. Angell and E. Sare, *J. Chem. Phys.*, 1968, **49**, 4713.
27 C. Monnin, M. Dubois, N. Papaiconomou and J. Simonin, *J. Chem. Eng. Data*, 2002, **47**, 1331–1336.
28 C. Angell and E. Sare, *J. Chem. Phys.*, 1970, **52**, 1058.
29 G. Walrafen, *J. Phys. Chem.*, 1990, **94**, 2237–2239.
30 R. Torre, P. Bartolini and R. Righini, *Nature*, 2004, **428**, 296–299.
31 P. Taborek, R. Kleiman and D. Bishop, *Phys. Rev. B*, 1986, **34**, 1835–1840.
32 C. Fecko, J. Eaves and A. Tokmakoff, *J. Chem. Phys.*, 2002, **117**, 1139–1154.
33 N. T. Hunt, A. A. Jaye and S. R. Meech, *Phys. Chem. Chem. Phys.*, 2007, **9**, 2167–2180.
34 Q. Zhong and J. T. Fourkas, *J. Phys. Chem. B*, 2008, **112**, 15529–15539.
35 D. A. Turton and K. Wynne, *J. Chem. Phys.*, 2009, **131**, 201101.
36 W. Murphy, *J. Chem. Phys.*, 1977, **67**, 5877–5882.
37 T. Fukasawa, T. Sato, J. Watanabe, Y. Hama, W. Kunz and R. Buchner, *Phys. Rev. Lett.*, 2005, **95**, 197802.
38 D. A. Turton and K. Wynne, *J. Chem. Phys.*, 2008, **128**, 154516.
39 S. Palese, S. Mukamel, R. Miller and W. Lotshaw, *J. Phys. Chem.*, 1996, **100**, 10380–10388.
40 K. Winkler, J. Lindner, H. Bursing and P. Vohringer, *J. Chem. Phys.*, 2000, **113**, 4674–4682.
41 K. Winkler, J. Lindner and P. Vohringer, *Phys. Chem. Chem. Phys.*, 2002, **4**, 2144–2155.
42 A. Scodinu and J. Fourkas, *J. Phys. Chem. B*, 2002, **106**, 10292–10295.
43 N. Ernsting, G. Photiadis, H. Hennig and T. Laurent, *J. Phys. Chem. A*, 2002, **106**, 9159–9173.
44 B. Ratajska-Gadomska, B. Bialkowski, W. Gadomski and C. Radzewicz, *Chem. Phys. Lett.*, 2006, **429**, 575–580.
45 N. T. Hunt, L. Kattner, R. P. Shanks and K. Wynne, *J. Am. Chem. Soc.*, 2007, **129**, 3168–3172.
46 N. Tao, G. Li, X. Chen, W. Du and H. Cummins, *Phys. Rev. A: At., Mol., Opt. Phys.*, 1991, **44**, 6665–6676.
47 Y. Amo and Y. Tominaga, *Phys. Rev. E: Stat. Phys., Plasmas, Fluids, Relat. Interdiscip. Top.*, 1998, **58**, 7553–7560.
48 D. A. Turton, J. Hunger, A. Stoppa, G. Hefter, A. Thoman, M. Walther, R. Buchner and K. Wynne, *J. Am. Chem. Soc.*, 2009, **131**, 11140–11146.
49 D. A. Turton, D. F. Martin and K. Wynne, *Phys. Chem. Chem. Phys.*, 2010, **12**, 4191–4200.
50 G. Giraud, C. Gordon, I. Dunkin and K. Wynne, *J. Chem. Phys.*, 2003, **119**, 464–477.
51 G. Giraud, J. Karolin and K. Wynne, *Biophys. J.*, 2003, **85**, 1903–1913.
52 E. Castner, Y. Chang, Y. Chu and G. Walrafen, *J. Chem. Phys.*, 1995, **102**, 653–659.
53 D. A. Turton, J. Hunger, A. Stoppa, A. Thoman, M. Candelaresi, G. Hefter, M. Walther, R. Buchner and K. Wynne, *J. Mol. Liq.*, 2011, **159**, 2–8.
54 D. A. Turton, M. Candelaresi, D. F. Martin and K. Wynne, 2011, **in preparation**.
55 E. Mamontov, *J. Phys. Chem. B*, 2009, **113**, 14073–14078.
56 J. Bertie and Z. Lan, *J. Chem. Phys.*, 1996, **105**, 8502–8514.
57 J. Max and C. Chapados, *J. Chem. Phys.*, 2001, **115**, 2664–2675.
58 C. Angell, K. Ngai, G. Mckenna, P. Mcmillan and S. Martin, *J. Appl. Phys.*, 2000, **88**, 3113–3157.
59 S. Sridhar and P. Taborek, *J. Chem. Phys.*, 1988, **88**, 1170–1176.
60 W. J. Ellison, *J. Phys. Chem. Ref. Data*, 2007, **36**, 1–18.
61 Y. Marcus, *J. Solution Chem.*, 2009, **38**, 513–516.
62 A. Omta, M. Kropman, S. Woutersen and H. Bakker, *Science*, 2003, **301**, 347–349.
63 K. Moller, R. Rey, M. Masia and J. Hynes, *J. Chem. Phys.*, 2005, **122**, 114508.
64 D. Laage and J. T. Hynes, *Proc. Natl. Acad. Sci. U. S. A.*, 2007, **104**, 11167–11172.
65 R. Mancinelli, A. Botti, F. Bruni, M. A. Ricci and A. K. Soper, *Phys. Chem. Chem. Phys.*, 2007, **9**, 2959–2967.
66 Y. Marcus, *Chem. Rev.*, 2009, **109**, 1346–1370.
67 L. Petit, R. Vuilleumier, P. Maldivi and C. Adamo, *J. Chem. Theory Comput.*, 2008, **4**, 1040–1048.
68 Y. Wei and S. Sridhar, *J. Mol. Liq.*, 1993, **56**, 259–273.
69 W. Wachter, S. Fernandez, R. Buchner and G. Hefter, *J. Phys. Chem. B*, 2007, **111**, 9010–9017.
70 P. U. Jepsen and H. Merbold, *J Infrared Millim Te*, 2010, **31**, 430–440.
71 Y. Suzuki, Y. Takasaki, Y. Tominaga and O. Mishima, *Chem. Phys. Lett.*, 2000, **319**, 81–84.
72 C. Angell and R. Bressel, *J. Phys. Chem.*, 1972, **76**, 3244–3253.
73 V. Trappe, V. Prasad, L. Cipelletti, P. Segre and D. Weitz, *Nature*, 2001, **411**, 772–775.

74 L. Xu, F. Mallamace, Z. Yan, F. W. Starr, S. V. Buldyrev and H. E. Stanley, *Nat. Phys.*, 2009, **5**, 565–569.
75 N. T. Hunt, A. R. Turner, H. Tanaka and K. Wynne, *J. Phys. Chem. B*, 2007, **111**, 9634–9643.
76 N. Hunt, A. Turner and K. Wynne, *J. Phys. Chem. B*, 2005, **109**, 19008–19017.
77 *Handbook of Chemistry and Physics*, CRC Taylor and Francis, 2006.
78 C. Angell and J. Tucker, *J. Phys. Chem.*, 1980, **84**, 268–272.
79 Y. Madokoro, O. Yamamuro, H. Yamasaki, T. Matsuo, I. Tsukushi, T. Kamiyama and S. Ikeda, *J. Chem. Phys.*, 2002, **116**, 5673–5679.
80 S. C. Santucci, L. Comez, F. Scarponi, G. Monaco, R. Verbeni, J.-F. Legrand, C. Masciovecchio, A. Gessini and D. Fioretto, *J. Chem. Phys.*, 2009, **131**, 154507.
81 M. E. Gallina, L. Bove, C. Dreyfus, A. Polian, B. Bonello, R. Cucini, A. Taschin, R. Torre and R. M. Pick, *J. Chem. Phys.*, 2009, **131**, 124504.

